Anal Bioanal Chem (2006) 384: 407–413
DOI 10.1007/s00216-005-0202-7

ORIGINAL PAPER

Bernd P. Möhrle · Karsten Köhler · Jan Jaehrling · Roland Brock · Günter Gauglitz

Label-free characterization of cell adhesion using reflectometric interference spectroscopy (RIfS)

Received: 16 August 2005 / Revised: 24 October 2005 / Accepted: 24 October 2005 / Published online: 1 December 2005

Abstract Reflectometric interference spectroscopy (RIfS) is a label-free, time-resolved technique for detecting interactions of molecules immobilized on a surface with ligands in solution. Here we show that RIfS also permits the detection of the adhesion of tissue culture cells to a functionalized surface in a flow system. Interactions of T cells with other leukocytes or epithelial cells of blood vessels are crucial steps in the regulating immune response and inflammatory reactions. Jurkat T cell leukemia cells rapidly attached to a transducer functionalized with a monoclonal antibody directed against the T cell receptor (TCR)/CD3 complex, followed by activation-dependent cell spreading. RIfS curves were obtained for the Jurkat derivative JCaM 1.6 (which lacks the key signaling protein Lck), cells preincubated with cytochalasin D (an inhibitor of actin polymerization), and for surfaces functionalized with an antibody directed against the coreceptor CD28. These curves differed with respect to the maximum signal and the initial slope of the increase in optical thickness. The testing of chemical inhibitors, cell surface molecules and gene products relevant to a key event in T cell immunity illustrates the potential of label-free techniques for the analysis of activation-dependent cell-surface contacts.

Keywords Cell assay · Drug development · Reflectometric interference spectroscopy (RIfS) · Label-free detection · T cell activation

The first two authors contributed equally to this paper

B. P. Möhrle (✉) · J. Jaehrling · G. Gauglitz
Institute of Physical and Theoretical Chemistry,
Eberhard-Karls-University of Tübingen,
Auf der Morgenstelle 8,
72076 Tübingen, Germany
e-mail: bernd.moehrle@ipc.uni-tuebingen.de
Tel.: +49-7071-2974668

K. Köhler · R. Brock
Department of Molecular Biology,
Institute for Cell Biology,
Eberhard-Karls-University of Tübingen,
Auf der Morgenstelle 15,
72076 Tübingen, Germany

Introduction

Cell–cell contacts are mediated through specific receptors that, in addition to establishing a physical link between cells, also act as signal-transducing molecules. Due to the significance of cell–cell interactions in health and disease there is a keen interest in the development of analytical techniques that enable the analysis of contacts with respect to kinetics, strengths and the underlying signaling processes. Reflectometric interference spectroscopy (RIfS) is a label-free, time-resolved technique that is able to detect biomolecular interactions of molecules immobilized on the surface of a transducer with analytes in solution ([1]; see Fig. 1). The binding of the analyte leads to an increase in the so-called optical thickness of the transducer-bound layer of molecules. This increase in thickness results in a change in the interference spectrum of light reflected at its boundaries. In contrast to surface plasmon resonance spectroscopy (SPR), the RIfS method is temperature-independent [2] and has a higher depth of penetration into the solution (about 300 nm for SPR and up to 40 μm for RIfS, depending on the wavelength) [3]. RIfS has been employed to measure the interaction kinetics of a variety of biomolecular interactions such as antibodies [4], biotin [5] and peptides [6]. The RIfS set-up is described in detail in the work of Schmitt et al. [7]. Despite their potential for detecting interactions of molecules, cellular applications have been limited. SPR has been used to analyze the adhesion of bacteria [8, 9] and erythrocytes [10] to surfaces. So far label-free techniques have not been used for the analysis of activation-dependent cellular interactions. Moreover, there is little information on the relationship of the signal to the molecular and morphological characteristics of a cell in contact with the transducer.

In the immune system, and especially in the immune surveillance performed by T lymphocytes, cell–cell con-

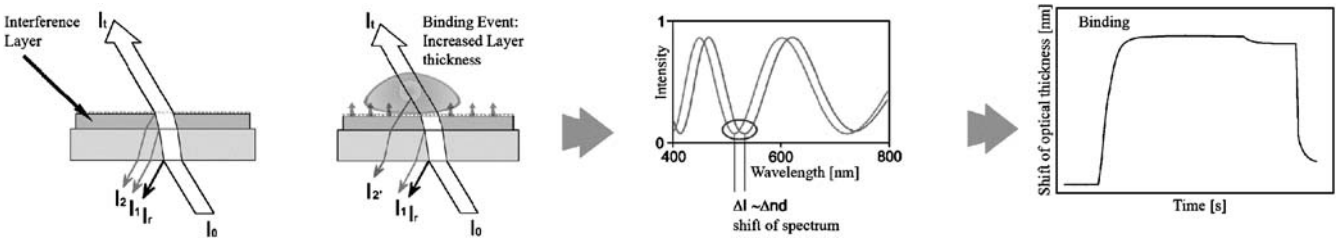

Fig. 1a–e Scheme of RIfS. The *left part* of the scheme shows how the reflected beams superimpose and how the optical thickness of the transducer changes during binding onto the surface. The *right part* shows the change in the characteristic interference spectrum and how this shift is transformed into a binding curve

tacts play a key role: T cells continuously circulate in the blood and lymphatic system, and engage in transient contacts with other cells mediated by interactions of their T cell receptors (TCR) with major histocompatibility complex (MHC)–peptide complexes on the target cell, and by interactions with other surface receptors [11]. The molecular mechanisms of contact formation between T cells and antigen-presenting cells have been investigated in great detail under static conditions (in the absence of flow). Activation of a T cell is a function of the affinity of the interaction, the density of specific MHC–peptide complexes on the cell surface, and the differentiation and activation state of the T cell [12]. Activation of cytotoxic T cells leads to the killing of a target cell and cytokine expression; T helper cells interact with professional antigen-presenting cells and contribute to the orchestration of an immune response. The cytokine-mediated guidance of T cells to their targets proceeds via adhesion-molecule contacts to the surface of the blood vessel epithelia, followed by active migration of the cells into the surrounding tissue [13, 14].

In order to better understand the events that precede T cell activation, such as extravasation, approaches that enable an analysis of T cell contacts under flow conditions are required. Ideally, such approaches should simultaneously provide information on the kinetics of an intercellular interaction and the cellular response. In drug development, such analyses will provide the basis for the screening of compounds that interfere with contact formation of T cells and will therefore be useful in the identification of immunomodulatory compounds.

Here, we demonstrate the application of RIfS to the analysis of T cell contacts and activation in a flow system. With ligand-functionalized surfaces, T cells form contacts that vary in intimacy and contact area depending on the nature of the ligand and the cell activation [15]. T cells are therefore also especially suited to evaluating the degree to which cellular responses to different stimuli can be discriminated based on a RIfS signal. Transducers were functionalized with different antibodies that served as well established and well defined stimuli. Antibodies directed against the CD3ε chain of the TCR/CD3 complex represent a strong T cell stimulus. The contact of T cells with anti-CD3-functionalized surfaces leads to a rapid spreading of cells on the surface within 2–5 minutes [16]. This process depends on the reorganization of the actin cytoskeleton and thus can be completely inhibited by the addition of 10 μM cytochalasin D, an inhibitor of actin polymerization [17]. Surfaces functionalized with antibodies directed against the CD28 coreceptor were believed to mediate specific T cell attachment, but instead of cell spreading the formation of small "microspikes" was observed [18]. Characteristic RIfS curves were obtained for Jurkat T cell leukemia cells perfused over anti-CD3- and anti-CD28-functionalized transducers and for cells inhibited with cytochalasin D and cells lacking the CD3-dependent upstream kinase Lck. Correlation of the results obtained by the label-free technology with those obtained by fluorescence microscopy yielded the morphological basis for these findings.

Experimental section

Chemicals

3-(Glycidyloxypropyl)trimethoxysilane (GOPTS) was purchased from Fluka, Neu-Ulm, Germany. Bovine serum albumin (BSA) was purchased from Sigma-Aldrich Chemie, Steinheim, Germany. Common chemicals of analytical grade were purchased from Sigma-Aldrich or Merck, Darmstadt, Germany. Cytochalasin D was purchased from Sigma-Aldrich and added from an aqueous solution to a final concentration of 10 μM. Cell viability after incubation with the inhibitor was validated using an MTT assay (not shown).

Tissue culture

The human T cell leukemia cell line Jurkat [19, 20] and the Lck-deficient derivative JCaM 1.6 [21] were cultivated in RPMI 1640 (PAN, Aidenbach, Germany) supplemented with 10% fetal calf serum (FCS; PAN). Expression of CD3 and CD28 surface antigens was validated using anti-CD3 (clone OKT3) and anti-CD28 (clone 9.3; both antibodies were kindly provided by G. Jung, Institute for Cell Biology, Tübingen, Germany) at a concentration of 2 μg/ml with subsequent detection by flow cytometry (BD FACSCalibur System, Becton Dickinson, Heidelberg, Germany) using an Alexa 488 goat anti-mouse secondary antibody (2 μg/mL). Cells were incubated with the antibodies for 1 h at 4 °C each.

Reflectometric interference spectroscopy (RIfS)

RIfS-transducer chips of 1 mm D 263 glass with layers of 10 nm Nb_2O_5 and 330 nm SiO_2 were purchased from Unaxis Balzers AG, Balzers, Liechtenstein. For functionalization, the RIfS-transducer chips were first cleaned in 1 M NaOH for 2 min, washed with tap water, and the surfaces were cleaned and mechanically dried with KIMTECH tissues (Kimberly-Clark, Reigate, UK). Then the transducer chips were treated with freshly prepared Piranha solution (mixture of 30% hydrogen peroxide and concentrated sulfuric acid at a ratio of 2:3 (v/v); Caution: Highly aggressive!) for 30 min in an ultrasonic bath to activate the silanol groups. After rinsing with Milli-Q water and drying in a nitrogen stream, the surface was immediately activated for protein binding by incubation with GOPTS for 1 h. Thereafter the surface was cleaned with water-free acetone and dried in a nitrogen stream. Antibody solutions (20 μg/mL in PBS) were added onto the activated transducer surface and incubated for 16 h at 4 °C. The same antibody clones were used for functionalization as for the detection of surface antigens. Before assembly into the flow cell, the transducers were rinsed with Milli-Q water and thoroughly dried in a nitrogen stream. Samples were handled with an Automated Sample Injection Analyser - ASIA (Ismatec, Wertheim-Mondfeld, Germany). Samples were perfused over the transducer in a continuous flow of 20 μL/min. First, FCS-free RPMI 1640 medium was pumped over the transducer until the signal showed no further drift. Then the transducer was blocked by perfusion of a solution of 0.1% BSA in PBS until, again, the signal showed no further drift.

The time for a complete measurement of cell adhesion and spreading was 2500 s. The first 120 s of serum-free RPMI 1640 medium was pumped over the transducer. Then, for 1800 s the cell suspension (with a density of 5×10^5 cells/mL), in serum-free medium in the absence or presence of inhibitor, was pumped through the flow cell. Finally, RPMI 1640 medium was pumped through the flow cell for the remainder of the measurement interval. The initial slope of the RIFS curve corresponds to the average increase in optical thickness between the 250 s and 350 s time points.

Spreading of cells on antibody-functionalized coverslips

For analysis of cell spreading by fluorescence microscopy, the anti-CD3 and anti-CD28 antibodies were immobilized on glass slides functionalized with GOPTS in the same way as the RIfS transducers. Solutions of antibodies (20 μg/mL in PBS) were incubated on the coverslips for 16 h at 4 °C, followed by three washes with PBS, and blocked with 0.1% BSA for 1 h.

Cells were added to antibody-functionalized coverslips at a density of 5×10^5 cells/mL in serum-free RPMI at 37 °C. In order to assess the effect of the inhibition of actin polymerization on cell spreading, cells were preincubated for 15 min with 10 μM cytochalasin D. For immunofluorescence, cells were fixed on the coverslips after 20 min of stimulation with paraformaldehyde (PFA, 3.7% in PBS), first for 10 min at 4 °C, then for 15 min at room temperature. In order to visualize the spreading of the cells on the surface, the surface not shaded by adherent cells was visualized using an Alexa546-labeled anti-mouse antibody (4 μg/ml in PBS, BSA (0.1%), Molecular Probes, Eugene, OR) directed against the immobilized stimulatory anti-CD3 and anti-CD28 antibodies. Following incubation with antibody for 30 min at room temperature, samples were washed and permeabilized with saponin buffer (PBS containing saponin (0.1%, Sigma) and BSA (0.1%)). Actin was detected using Cy5-labeled phalloidin (5 U/sample, Molecular Probes) in saponin buffer. After washing three times with saponin buffer, samples were fixed once more with PFA for 15–20 min, washed three times with PBS, and embedded in MOWIOL [22]. The area of the surface shielded by the cell against staining with the secondary antibody was quantitated using ImageProPlus (Media Cybernetics, Silver Spring, MD, USA). Immunofluorescence microscopy was performed on an inverted LSM 510 confocal laser scanning microscope (Carl Zeiss, Göttingen, Germany) using a Plan-Neofluar 40×0.75 NA lens for nonconfocal and a C-Apochromat 63×1.3 NA oil immersion lens for confocal imaging (both from Carl Zeiss). Alexa 546 and Cy5 fluorescence were detected using a filter set consisting of an HFT UV/488/543/633 beam splitter in combination with an NFT 635 VIS beam splitter and a BP 560-615 detection filter for Alexa 546, and an LP650 long-pass filter for Cy5.

Results and discussion

Spreading of T cell leukemia cells on antibody-functionalized surfaces

Antibody-functionalized coverslips represent a well-defined T cell stimulus that enables the analysis of T cell signal transduction and the effect of chemical inhibitors under highly controlled conditions [15, 16]. First, the spreading of Jurkat T cells on antibody-functionalized surfaces was determined using immunofluorescence microscopy in a stopped flow protocol. Antibodies were immobilized on epoxy-activated glass surfaces in order to closely mimic the conditions used for to immobilize antibodies on the RIfS transducers. The high reflectivity compromised the analysis of cell contacts on RIfS transducers using fluorescence microscopy. Cells were allowed to settle on antibody-functionalized coverslips and were fixed after 20 min. On anti-CD3-functionalized coverslips, the formation of tight contacts with the surface was observed for most cells, and about 15% of the cells showed a spreading of more than twice the cell diameter (Fig. 2a). The detection of surface contacts was based on a recently developed protocol according to which cells are fixed but not permeabilized [15]. In the presence of tight contacts, a fluorescently labeled secondary antibody directed against

the antibody used for cell stimulation can only stain the part of the surface of the coverslip that is not shielded by the cells.

In contrast, the cells attached to the anti-CD28 functionalized surface, but spreading and contact formation were strongly reduced (Fig. 2b). The difference in cell spreading was also evident after phalloidin staining of the actin cytoskeleton. On the anti-CD3-coated surface strong polymerization of actin was present along the leading edge of the spread cells. Little actin was present in the contact zone (Fig. 2a). On anti-CD28-coated surfaces, cells adhered tightly but no spreading was observed, and the contact zone was poor in polymerized actin. JCaM 1.6 cells, a Jurkat derivative cell line deficient in the CD3-dependent upstream kinase Lck, showed a strong reduction in cell-spreading, and polymerized actin was distributed around the periphery of the cells, especially in the contact zone (Fig. 2c). Pretreatment of cells with the inhibitor of actin polymerization cytochalasin D completely abolished firm cell attachment and spreading and inhibited the localization of the actin to contact sites (Fig. 2d). The cells showed little contact with the surface. Finally, the cells attached to BSA but no spreading was observed (Fig. 2e), and actin was evenly localized in the membrane-proximal region of the cell. In conclusion, each surface led to a distinct pattern in spreading and reorganization of the actin cytoskeleton.

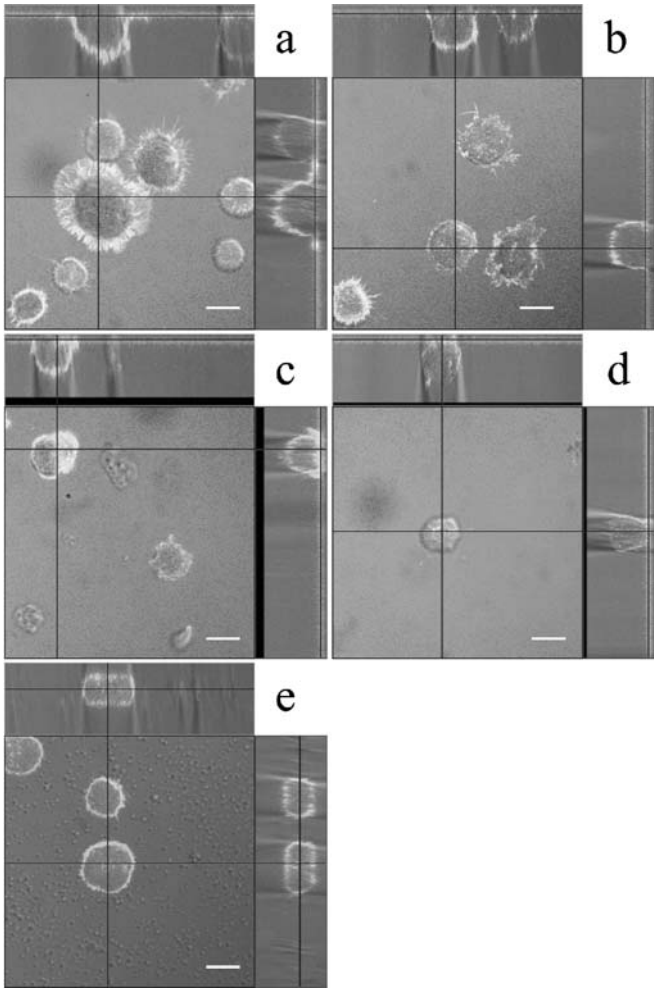

Fig. 2a–e Contact formation for cells on antibody- and BSA-functionalized surfaces. Jurkat cells (**a**, **b**, **d**, **e**) or the Lck-deficient Jurkat derivative JCaM 1.6 (**c**) were exposed to coverslips functionalized with anti-CD3 antibodies (**a**, **c**, **d**), with anti-CD28 antibodies (**c**) or BSA (**e**) in the absence (**a**–**c**, **e**) or presence (**d**) of the inhibitor of actin polymerization cytochalasin D (10 μM). Cells were allowed to establish contacts for 20 min before fixation. The immunofluorescence staining of the antibody used for surface functionalization is shown in *gray*; the Cy5-phalloidin staining of filamentous actin is shown in *light gray*. Cells were fixed but not permeabilized. For this reason, parts of the surface in close contact with a cell are not accessible to the secondary antibody. In each panel, an x-y section and orthogonal projections through the confocal image stack along the indicated lines are shown. The bar corresponds to 10 μm

Label-free detection of cell attachment by RIfS Having established that wild-type Jurkat cells showed different phenotypes on anti-CD3-, anti-CD28- and BSA-coated surfaces, the adhesion of these cells to functionalized RIfS transducers was then detected in a flow system with a flow rate of 20 μL per minute. The RIfS signal showed similar general characteristics on each type of surface. In each case, a steep initial increase was followed by a second phase of a slower increase. For the anti-CD3-coated surface, the maximum increase in optical thickness at 2000 s was about 1.5 times as high as the one detected for the anti-CD28 and BSA-coated surfaces. Once the perfusion of the cell suspension was stopped and the flow cell was perfused with just medium instead, very similar absolute decreases in optical thickness were observed in each case (Fig. 3).

The signals for the adhesion to anti-CD3 and anti-CD28 surfaces were referenced against the nonspecific adhesion on BSA surfaces at the 2000 s time point (Fig. 4). The

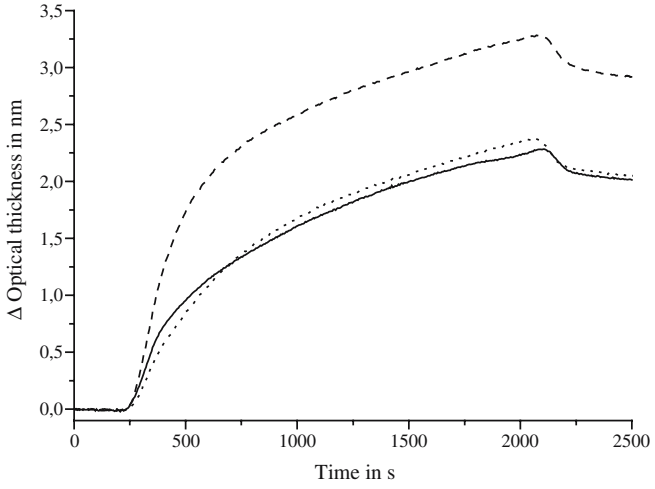

Fig. 3 RIfS measurements of the adhesion of Jurkat T cells to different surfaces. 5×10^5 Jurkat cells/mL were pumped through a flow chamber at a flow of 20 μL/min over various functionalized transducer surfaces. The time-dependent changes in optical thickness for Jurkat attachment to anti-CD3- (*dashed line*), Jurkat to anti-CD28- (*solid line*) and Jurkat to BSA-functionalized surfaces (*dotted line*) are plotted

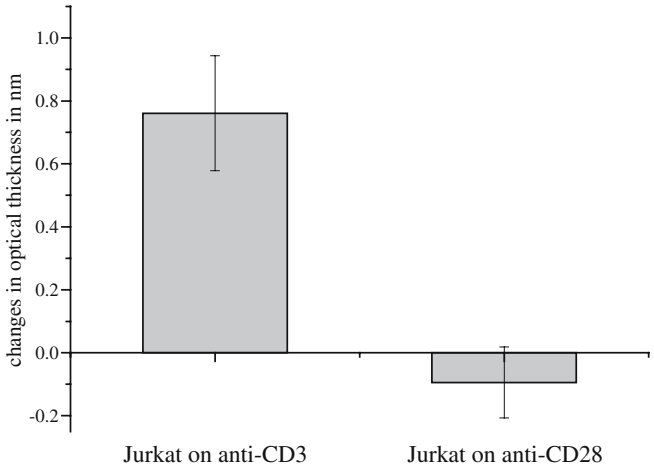

Fig. 4 Bar chart of the RIfS signal for the attachment of Jurkat cells to anti-CD3- (n=4) and anti-CD28- (n=3) functionalized surfaces referenced against nonspecific binding to BSA at the 2000 s time point. The difference in signal between both surfaces is significant (t-test, P=0.05)

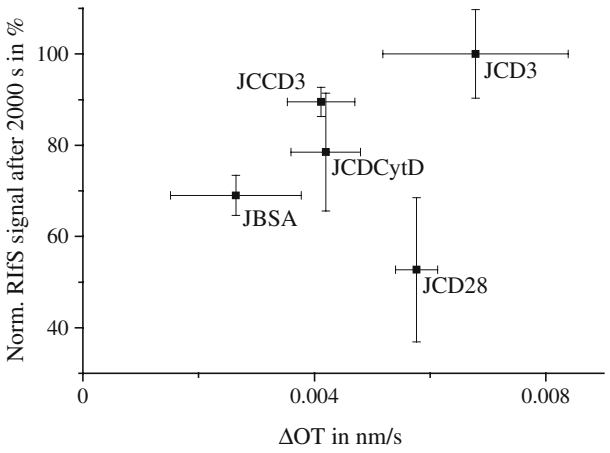

Fig. 5 Correlation between the maximum optical thickness after 2000 s and the initial slopes of the tangents to the optical thickness curves (ΔOT). *JCD3*, *JCD28* and *JBSA* indicate Jurkat cells adhering to a surface functionalized with anti-CD3, anti-CD28 antibodies or BSA, *JCCD3* the Lck-deficient JCaM 1.6 cells on an anti-CD3 surface, and *JCD3CytD* Jurkat cells pretreated with 10 μM of the actin inhibitor cytochalasin D before perfusion over an anti-CD3-functionalized surface. The average values of the maximal optical thickness were normalized to the spreading of Jurkat cells on anti-CD3-coated transducers

RIfS signal for the adhesion of the T cells to both surfaces was significantly different (t-test, P=0.05). This high reproducibility was obtained despite the use of different transducers, freshly prepared cell suspensions for each experiment and the fact that a complete series of measurements could not always be performed in direct succession. This may also account for the rather high variability in the RIfS signal. Interestingly, on anti-CD28-coated surfaces, the maximum optical thickness was slightly but reproducibly smaller than on BSA-coated surfaces.

In addition to the maximum increase in optical thickness, a comparison of the initial slopes of the RIfS curves (ΔOT) yielded additional information. Even though the maximum increase in the optical thickness was smaller on the anti-CD28-coated surface than on the BSA control, the initial increase in the RIfS curve for the Jurkat cells was much higher on the anti-CD28-coated surface ($\Delta OT=(5.8\pm0.4)\times10^{-3}$ nm/s) than on the BSA-coated surface ($\Delta OT=(2.6\pm1.3)\times10^{-3}$ nm/s) (Fig. 3). The increase in optical thickness for the anti-CD3-functionalized surface had the highest slope ($\Delta OT=(6.8\pm1.6)\times10^{-3}$ nm/s).

Characterization of mutant cell lines and chemical inhibitors

The initial measurements demonstrated that RIfS permitted discrimination of the adhesion behavior of the Jurkat T cells on surfaces functionalized with antibodies that either induce a strong activation of cell spreading or mediate specific adhesion but little spreading, and on surfaces functionalized with BSA that induce only nonspecific interactions.

We therefore also explored the extent to which the label-free time-resolved detection of cell attachment permitted characterization (i) of the adhesion behaviors of different cell lines and (ii) of the effects of pharmacological inhibitors of cell attachment and spreading. Each condition was characterized with respect to the maximum increase in optical thickness and the initial slope of the RIfS curve (Fig. 5). For JCaM 1.6 cells perfused over the anti-CD3-coated surface, the maximum RIfS signal was reduced by 11% in comparison to the signal from wild-type Jurkat cells (Table 1) but was still higher than the one for the wild-type cells on BSA- and on anti-CD28-coated surfaces. The initial slope of the RIfS curve ($\Delta OT=(4.1\pm0.6)\times10^{-3}$ nm/s) was lower than the one for Jurkat cells on anti-CD28-functionalized coverslips.

The spreading of the Jurkat T cells on the immobilized anti-CD3 antibody surface is an actin-dependent process. For this reason, the inhibitor of actin polymerization cytochalasin D was used to evaluate the applicability of RIfS to the detection of pharmacological interventions. Cytochalasin D treatment does not inhibit the attachment of cells to anti-CD3-coated surfaces or the formation of signaling clusters, but it does completely abolish cell spreading [15]. Preincubation of cells with cytochalasin D

Table 1 Reduction in the RIfS signal for the 2000 s time point relative to the signal from Jurkat cells on the anti-CD3 antibody surface (n=3)

	Reduction in the RIfS-signal in %
Jurkat cells on anti-CD28 antibody surface	47.3±15.8
Jurkat cells on BSA surface	31.0±4.4
Jurkat cells on anti-CD3 antibody surface pretreated with 10 μM cytochalasin D	21.5±12.9
JCaM 1.6 cells on anti-CD3 antibody surface	11.5±3.2

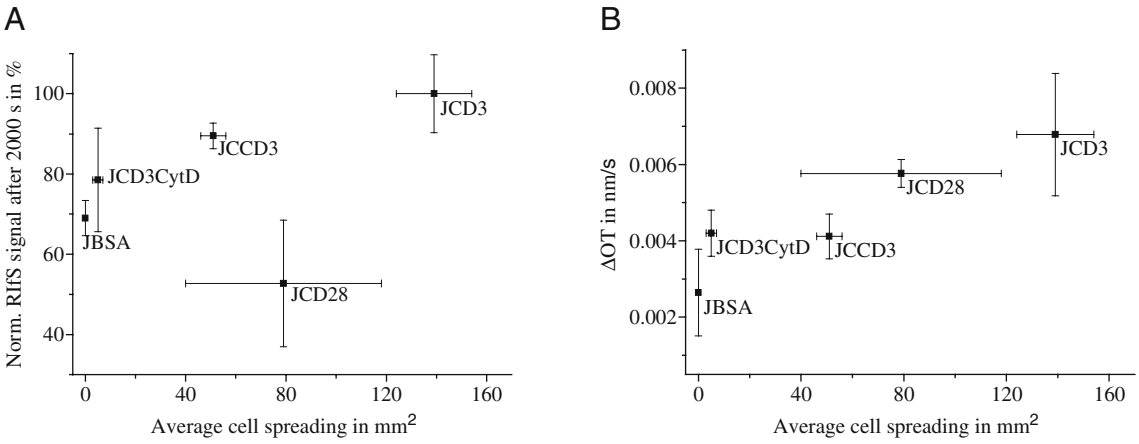

Fig. 6a–b Correlation between RIfS and immunofluorescence microscopy. **a** Maximum RIfS signal after 2000 s versus the average cell spreading, determined by immunofluorescence microscopy and digital image processing. **b** Slopes of the tangents to the optical thickness curves (ΔOT) versus average cell spreading, determined by immunofluorescence microscopy

led to a reduction in the maximum RIfS-signal by 21.5%± 12.9% (Table 1). Interestingly, the initial slope of the RIfS curve ($\Delta OT=(4.2\pm0.6)\times10^{-3}$ nm/s), was in the same range as the one observed for JCaM 1.6 cells. Similar to the JCaM 1.6 cells, the maximum increase in optical thickness was higher for cytochalasin D-treated cells (even though the initial kinetics of attachment were slow) than the one for Jurkat cells on anti-CD28-coated surfaces.

Correlation between kinetics of cell attachment and cell spreading The time-resolved RIfS measurements yielded information on the kinetics of T cell attachment and spreading in the presence of flow. We therefore asked whether correlations existed between the behaviors of the cells in the flow system and in the stopped flow configuration. Interestingly, the initial kinetics of cell attachment rather than the maximum RIfS signal showed a strong positive correlation with the cell spreading, as determined by immunofluorescence microscopy (Fig. 6). The lower maximum RIfS signal observed despite the larger average area for Jurkat cells on anti-CD28-coated surfaces in comparison to JCaM 1.6 cells, cytochalasin D-treated cells and cells on BSA is a nontrivial result that cannot be explained by the RIfS analysis alone.

In the analysis of cell attachment and spreading, three factors may contribute to an increase in optical thickness: (i) cell attachment; (ii) spreading of an already attached cell, and; (iii) the refractive index in the contact area. The higher maximum optical thickness for the latter three cases may readily be explained by the fluorescence microscopy data: For each condition, the number of cells was the same even though a loss of cells during fixation and washing cannot be fully excluded. However, in contrast to the anti-CD28-coated surface, for the JCaM 1.6 cells on an anti-CD3-coated surface and the Jurkat cells on BSA, a strong enrichment of filamentous actin in the contact area was observed. The higher RIfS signal is therefore most likely a consequence of the local enrichment of protein.

Using the combination of results from immunofluorescence microscopy and RIfS in particular, it is now possible to distinguish between modes of binding in which (i) unspecific contacts are formed, as for the BSA-coated surface, (ii) contacts establish quickly and induce firm attachment but no cell spreading even though contacts are less intimate/or the membrane proximal region is less enriched in protein, as for the anti-CD28-coated surfaces, (iii) contacts establish slowly and cells do not spread or spread only in little extent, but the contact area still has a high optical thickness, as for the JCaM 1.6 cells and possibly for cytochalasin-treated Jurkat cells, and where (iv) contacts establish quickly and cells spread strongly, as for Jurkat cells on the anti-CD3-coated surfaces.

Conclusion

The results demonstrate that the label-free RIfS technique permits the various states of cell adhesion and activation in a flow system to be distinguished in a sensitive manner. Cells responded differently to surfaces functionalized with different stimulatory antibodies. Moreover, cells lacking a signaling protein and cells treated with an inhibitor of cell spreading yielded characteristic signatures based on kinetics and maximum optical thickness. Correlation with the results obtained by RIfS with fluorescence imaging provided an explanation for the increases in optical thickness observed for the individual conditions, a prerequisite for the wider application of label-free techniques in cell biology. Remarkably, the cell spreading observed in a stopped-flow protocol correlated with the initial increase in the RIfS signal rather than with the maximum increase in optical thickness. There is evidence that the association kinetics of the TCR with the MHC peptide complex is a major determinant for the activation of a T cell in T cell receptor-dependent signal transduction [23]. The flow system and especially the correlation of the dynamic data with fluorescence imaging, as exemplified in this contribu-

tion, should enable these questions to be addressed in a highly robust experimental set-up. Finally, the analysis of T cell attachment in the presence of flow enables compounds that interfere with T cell interactions in a flow system to be screened for.

Acknowledgements We thank Ludger Grosse-Hovest and Gundram Jung for providing antibodies. The JCaM 1.6 cell line was a kind gift from Claus Belka. Roland Brock gratefully acknowledges financial support from the Volkswagen Foundation (Nachwuchsgruppen an Universitäten). Jan Jaehrling and Bernd Möhrle were participants of the research training group (Graduiertenkolleg) 8 "Quantitative Analysis and Characterisation of Pharmaceutically and Biochemically relevant Substances", and Karsten Köhler is a member of the Graduiertenkolleg 794 "Cellular Mechanisms of Immune-Associated Processes", both funded by the Deutsche Forschungsgemeinschaft (DFG) at the Eberhard Karls University of Tübingen.

References

1. Piehler J, Brecht A, Giersch T, Hock B, Gauglitz G (1997) J Immunol Methods 20:189–206
2. Pröll F, Möhrle B, Kumpf M, Gauglitz G (2005) Anal Biochem 382:1889–1894
3. Hecht E (1987) Optics, 2nd edn. Addison Wesley, Boston
4. Proll G, Kumpf M, Mehlmann M, Tschmelak J, Griffith G, Abuknesha R, Gauglitz G (2004) J Immunol Methods 292:35–42
5. Piehler J, Brecht A, Gauglitz G (1996) Anal Chem 68:139–143
6. Kröger K, Bauer J, Fleckenstein B, Rademann J, Jung G, Gauglitz G (2002) Biosens Bioelectron 17:937–944
7. Schmitt HM, Brecht A, Piehler J, Gauglitz G (1997) Biosens Bioelectron 12:809–816
8. Pourshafie MR, Marklund BI, Ohlson S (2004) J Microbiol Methods 58(3):313–320
9. Toby A, Jenkins A, Ffrench-Constant R, Buckling A, Clarke DJ, Jarvis K (2004) Biotechnol Prog 20:1233–1236
10. Quinn JG, O'Neill S, Doyle A, McAtamney C, Diamond D, MacCraith BD, O'Kennedy R (2000) Anal Biochem 281 (2):135–143
11. van der Merwe PA, Davis SJ (2003) Annu Rev Immunol 21:659–684
12. Healy JI, Goodnow CC (1998) Annu Rev Immunol 16:645–670
13. Mackay CR (2001) Nat Immunol 2(2):95–101
14. Engelhardt B, Wolburg H (2004) Eur J Immunol 34(11):2955–2963
15. Köhler K, Lellouch AC, Vollmer S, Stoevesandt O, Hoff A, Peters L, Rogl H, Malissen B, Brock R (2005) Chembiochem 6 (1):152–161
16. Bunnell SC, Kapoor V, Trible RP, Zhang W, Samelson LE (2001) Immunity 14(3):315–329
17. Parsey MV, Lewis GK (1993) J Immunol 151(4):1881–1893
18. Salazar-Fontana LI, Barr V, Samelson LE, Bierer BE (2003) J Immunol 171(5):2225–2232
19. Gillis S, Watson J (1980) Biochemical J Exp Med 152 (6):1709–1719
20. Weiss A, Wiskocil RL, Stobo JD (1984) J Immunol 133 (1):123–128
21. Straus DB, Weiss A (1992) Cell 70(4):585–593
22. Osborn M, Weber K (1982) Meth Cell Biol 24:97–132
23. Gonzalez PA, Carreno LJ, Coombs D, Mora JE, Palmieri E, Goldstein B, Nathenson SG, Kalergis AM (2005) Proc Natl Acad Sci USA 102(13):4824–4829